

Off-design model of concentrating solar power plant with thermochemical energy storage based on calcium-looping

Cite as: AIP Conference Proceedings 2126, 210006 (2019); <https://doi.org/10.1063/1.5117755>
Published Online: 26 July 2019

Carlos Ortiz, Marco Binotti, Matteo C. Romano, José Manuel Valverde, and Ricardo Chacartegui



View Online



Export Citation

ARTICLES YOU MAY BE INTERESTED IN

[Limestone calcination-carbonation in a fluidized bed reactor/receiver for thermochemical energy storage applications](#)

AIP Conference Proceedings 2126, 210008 (2019); <https://doi.org/10.1063/1.5117757>

[Calcium, strontium and barium carbonate mixtures for calcination-carbonation thermochemical energy storage](#)

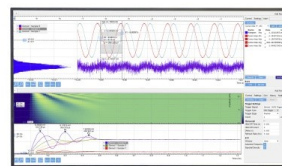
AIP Conference Proceedings 2126, 210002 (2019); <https://doi.org/10.1063/1.5117751>

[Fe-doped \$\text{CaMnO}_3\$ for thermochemical heat storage application](#)

AIP Conference Proceedings 2126, 210005 (2019); <https://doi.org/10.1063/1.5117754>

Challenge us.

What are your needs for
periodic signal detection?



Zurich
Instruments



Off-Design Model of Concentrating Solar Power Plant with Thermochemical Energy Storage Based on Calcium-Looping

Carlos Ortiz^{1, a)}, Marco Binotti², Matteo C. Romano², José Manuel Valverde¹ and Ricardo Chacartegui³

¹*Facultad de Física, Universidad de Sevilla, Avenida Reina Mercedes s/n, 41012 Sevilla, Spain*

²*Politecnico di Milano - Dipartimento di Energia, Via Lambruschini 4, 20156 Milano, Italy*

³*Escuela Técnica Superior de Ingeniería, Universidad de Sevilla, Camino de los descubrimientos s/n, 41092 Sevilla, Spain*

^{a)}Corresponding author: cortiz7@us.es

Abstract. Dispatchability is a key issue to increase the competitiveness of concentrating solar power plants. Thermochemical energy storage systems are a promising alternative to molten salt-based storage because of the higher energy storage density and the possibility of increasing the storage period. Among possible thermochemical systems, the Calcium-Looping process, based on the multicycle calcination-carbonation of CaCO_3 , is a main candidate to be integrated as energy storage system within a scenario of massive deployment of concentrating solar power plants. The present manuscript goes beyond previous works by developing an off-design model of the system that leads to a more accurate discussion on system size and plant efficiency. A capacity factor as high as 58% is calculated with lower mass of stored products than in commercial solar plants while the calculated solar-to-electric daily efficiency varies between 17.1% and 20.1%. Simulation results suggest an interesting attractive potential of the Calcium-Looping integration.

INTRODUCTION

The number of Concentrating Solar Power (CSP) plants throughout the world has notably increased in the last 10 years, reaching a total installed capacity worldwide of about 5 GW_e [1]. However, for a massive deployment of CSP plants, significant investment cost reductions and efficiency increase are needed in order to achieve competitive levelized cost of electricity. The present work focuses on the integration of the Calcium-Looping (CaL) process as Thermochemical Energy Storage (TCES) system in CSP plants. The CaL process, based on the cyclic calcination and carbonation of CaCO_3 , is also gaining attention in last years as post-combustion CO_2 capture process [2]. Concentrated solar radiation is used to carry out the endothermic calcination reaction which produces CaO and CO_2 . The products are stored separately and, when energy is demanded, these are brought together to release the stored energy through the carbonation (exothermic) reaction. The CSP-CaL process is fully aligned with the priority research lines in CSP technology [3]. Dispatchability can be improved taking advantage of the high storage energy density of the system CaCO_3/CaO . Because the carbonation reaction can take place in a pure CO_2 atmosphere at temperatures as high as $\sim 890^\circ\text{C}$ at ambient pressure (and even higher temperatures by increasing the reactor pressure), high temperature heat is introduced in the thermodynamic cycle, which leads to a thermal-to-power cycle efficiency superior to that of molten salt-based plants [4]. Moreover, cost and sustainability of CSP plants can be enhanced due to low cost, wide availability and non-toxicity of natural CaO precursors (i.e. limestone or dolomite).

The CaL process for TCES was already conceptualized in the late 1970s [5], while the first design of a reactor to carry out the solar calcination was developed in 1980 [6]. However, CSP-CaL process integration works have not been proposed until recently. Edwards et al. [7] analyzed a CSP-CaL integration scheme in which the heat produced in the carbonator reactor is used for power generation through a CO_2/air open cycle. As alternative, a regenerative

CO₂ closed Brayton cycle was proposed by Chacartegui et al. [4]. This scheme was further studied from an energy optimization point of view by Alovio et al. [8]. In a recent work [9], Ortiz et al. analyzed four novel configurations by considering high temperature solids storage, which simplifies the heat integration process while maintaining a high-energy storage potential. The present work goes beyond previous studies introducing an off-design plant analysis and a yearly analysis based on hour-by-hour calculations with real solar radiation data from Seville (Spain).

CSP-CAL PLANT

Figure 1 shows the conceptual CSP-CaL plant scheme, which was developed by Ortiz et al. [9]. The process starts with the decomposition of CaCO₃ in the solar calciner at 900°C. A closed cavity falling particle receiver is considered as solar calciner and full calcination is assumed [10]. CaO is stored at high temperature while the CO₂ produced by calcination is cooled down in a solids preheater (GS-HE1 in Fig. 1) after which a heat recovery steam generator (HRSG) is introduced. Thus, part of the heat recovered during CO₂ cooling is used as thermal input for a heat recovery steam power cycle designed as a simple Rankine cycle with moderate live steam conditions (400°C/40 bar). Later on, the cooled CO₂ stream is sent to the CO₂ power cycle for power production or compressed (HPS-COMP) and stored in a pressurized CO₂ vessel, depending the selected operation mode.

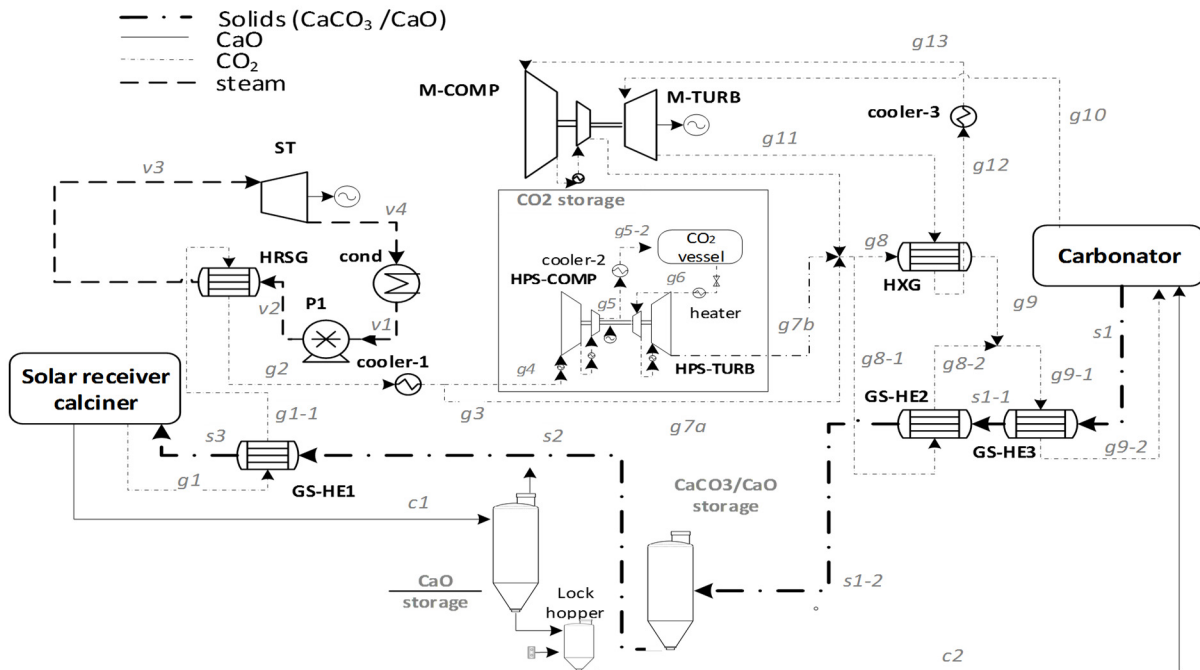


FIGURE 1. CSP-CaL plant scheme. Reproduced with permission from [9].

When energy production is demanded, CO₂ is extracted from the storage vessel and is fed into the carbonator along with CaO solids with which it reacts exothermically (carbonation) at 850°C and ambient pressure producing CaCO₃. The amount of CO₂ entering the carbonator (either coming from the storage tank, from the calciner side directly or mixing the two streams) is well above the stoichiometric ratio and the excess CO₂ is used as working fluid. Previously, the CO₂ entering the carbonator is preheated in several gas-gas (HXG, which acts as the regenerator of the Brayton cycle) and solids-gas (GS-HE2 and GS-HE3) heat exchangers. The hot CO₂ stream expands below atmospheric pressure (pressure ratio of 3) in the expander (M-TURB) of a regenerative Brayton cycle. The regenerated CaO suffers a progressive loss of carbonation activity as the number of cycles increases. In the present work, a residual value of CaO conversion (X) of 0.15 is assumed. The interested reader is referred to [9] where a CSP-CaL plant is described in detail and main assumptions considered in the modelling process are specified. The carbonator is modelled by assuming losses of 1% of the heat transferred and auxiliaries power consumption for all heat rejection systems is taken as a 0.8% of the heat rejected [11].

Because of the high temperature required for the calcination process, solar tower technology is the most adequate thanks to the high concentration ratio achievable. The CSP-CaL plant based on the scheme illustrated in Fig. 1 is modeled assuming $100 \text{ MW}_{\text{th}}$ as calciner net thermal input at design conditions. A preliminary solar field design is performed using SolarPILOT [12] at the summer solstice in Seville (Spain), assuming four $6\text{m}\times 6\text{m}$ targets corresponding to the entrances of four closed cavity receivers, similarly to the layout proposed in [13]. The receiver is modeled with a simplified approach assuming 80% absorptivity and 100 kW/m^2 thermal losses. Main inputs for the solar field design and obtained performance are reported in Table 1. The designed solar field (Fig. 2) counts 6081 heliostats and has an optical efficiency of 67.4%. A solar multiple (SM) equal to 2.7, as in other solar tower plants [14], is assumed.

TABLE 1. Main input for the design of the solar field using SolarPILOT and main results on the 21st of June in Seville.

Assumptions	Value	Results	Value
Number of cavities	4	Optical efficiency	0.674
Cavity aperture size, H×L (m)	6×6	Intercept factor	0.915
Cavity absorptivity	0.8	Cosine efficiency	0.816
Tower height (m)	100	Blocking efficiency	0.987
Field type	Surrounded	Solar Power (MW)	212.3
Minimum/Maximum field radius (m)	75/597	Power entering the cavities (MW)	143.1
Heliostats size, H×W (m × m)	6×6	Absorbed power (MW)	114.5
Heliostats total reflected image errors (mrad)	4.34	Power for calcination (MW)	100.1
Mirror reflectivity (-)	0.95		
Design DNI (W/m^2)	970		

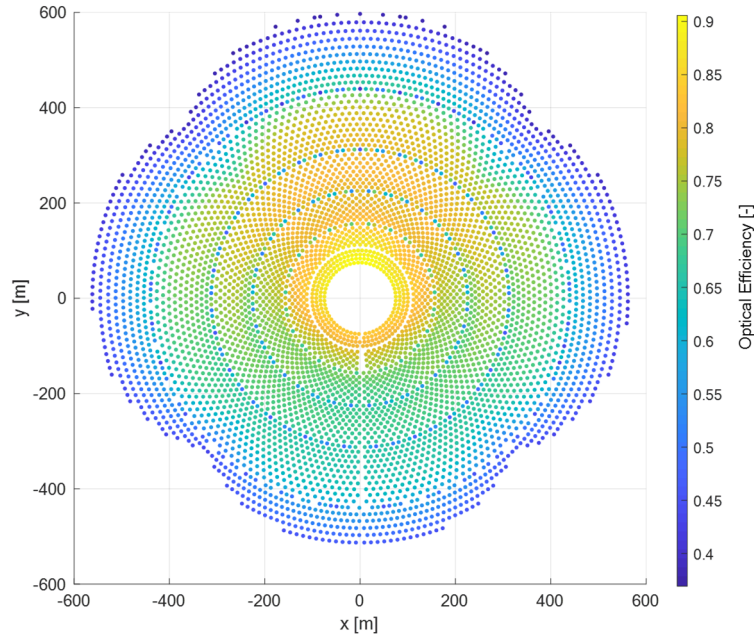


FIGURE 2. Solar field layout and heliostat optical efficiency on the 21st of June in Seville.

CaO and CaCO₃ solids vessels capacity are fixed to 3050 and 3409 tonnes, respectively, allowing power production from storage (at design conditions) for 16 hours. By considering packing density and solids porosity [9], a total storage volume of 3062 m³ for CaO and 2097 m³ for CaCO₃ are needed. Tanks volumes are evaluated later in the yearly simulation to corroborate that they guarantee a correct operation of the plant. Regarding the CO₂ storage, CO₂ isothermal tank is considered. The CO₂ tank is kept at 25°C and 75 bar by using a cooling system. Cylindrical pressure vessels made of chromium and molybdenum doped stainless steel could be an option to storage CO₂ under these conditions [15]. A tank of reduced size can be installed since CO₂ is stored at liquid conditions, albeit power

consumption would increase due to the need of a higher compression power and electric consumption for the cooling system. As design value, a pressurized CO₂ tank of 462 m³ is considered to produce power from storage for 16 hours.

Under design conditions (21st June at solar noon, DNI=970 W/m²) the solar field supplies about 100 MW to the calcination process leading to the production of 16.83 kg/s of CO₂ and of 21.42 kg/s of CaO. Since solids entering the calciner mostly consist of CaO (for the assumed low value of residual conversion in the carbonator X=0.15), the total amount of CaO exiting the solar calciner is 142.97 kg/s. According to the selected solar multiple of 2.7, a fraction of 1/2.7 of the produced CO₂ is directly sent to the CO₂ power cycle, while 1.7/2.7 is sent to the storage system. It is important to consider that, in contrast with the molten salt case, consumption of the storage auxiliaries has a strong impact on the overall energy balance due to the high storage compression power required. The higher the selected solar multiple, the lower is the system net power. In Table 2 main energy and mass flows are summarized for the design case, for a case with SM=1 and for the night mode.

TABLE 2. Main energy and mass fluxes for the CSP-CaL plant power block and storage systems. Names in *Italic* refer to fig.1.

Power Block + storage results			
	Design	Design SM=1	Night mode
Power for calcination (MW)	100	37.04	-
CO ₂ produced in the calciner, <i>g1</i> (kg/s)	16.83	6.23	-
CO ₂ to storage, <i>g4</i> (kg/s)	10.60	-	-
CO ₂ to power block, <i>g3</i> (kg/s)	6.23	6.23	-
Power Productions (MW)	32.81	30.87	30.86
CO ₂ storage turbine, <i>HPS-TURB</i> (MW)	-	-	1.12
Main CO ₂ turbine, <i>M-TURB</i> (MW)	29.74	29.74	29.74
Steam Turbine, <i>ST</i> (MW)	3.07	1.13	-
Power Consumptions (MW)	-20.95	-16.09	-15.47
Steam cycle pump, <i>PI</i> (MW)	-0.02	-0.01	-
Main CO ₂ compressor, <i>M-COMP</i> (MW)	-14.75	-14.75	-14.75
CO ₂ storage compressor, <i>HPS-COMP</i> (MW)	-3.74	-	-
Auxiliaries for heat rejection, calciner side (MW)	-0.12	-0.02	-
Auxiliaries for heat rejection, carbonator side (MW)	-0.13	-0.13	-0.13
Auxiliaries for solids transport calciner (MW)	-1.6	-0.59	-
Auxiliaries for solids transport carbonator (MW)	-0.59	-0.59	-0.59
Net Power (MW)	11.86	14.78	15.39

OFF-DESIGN PERFORMANCE MODELLING

Solar field performance as a function of the sun position (Azimuth and Zenith) has been computed using SolarPILOT (See Fig. 3a), where absorptivity and thermal losses in off-design conditions have been assumed as constant for the sake of simplicity.

The performance of the heat recovery steam cycle under off-design conditions has been calculated as a function of the ambient temperature and of the CO₂ mass flow from the calciner (*g1-1* stream in Fig. 1) by using Thermoflex® [16]. Figure 3b shows sensitivity analysis results for the CSP-CaL plant net power at partial-load for several ambient temperatures. The steam turbine inlet live steam temperature (400°C) and pressure (40 bar) are kept constant by means of an attemperator and of a nozzle control, respectively. Steam turbine efficiency is assumed to be constant. Pressure drops are calculated as a percentage of steam and CO₂ mass flows by introducing a flow resistance coefficient. HRSG is simulated by scaling exponentially the heat transfer coefficient value (exponent of 0.8 [17]) respect to the mass flow rate and considering thermal losses of 1% of the heat transferred by the CO₂. A multistage centrifugal pump with variable speed is considered.

All gas-solid heat exchangers are considered as open cyclonic preheaters and modeled by assuming a co-flow arrangement. For coolers and condensers, a constant $\Delta T=15^{\circ}\text{C}$ with ambient temperature is assumed. The regenerator

(HXG) is modelled by varying the overall heat transfer coefficient (U) scaling it potentially with the mass flow with an exponent of 0.8 [17]. Pressure drops used are obtained from [9]. As under design conditions, power consumption in off design for heat rejection is kept equal to 0.8% of the heat rejected from all coolers [11].

As control strategy, power production in the CO₂ power cycle is kept constant. This criterion imposes that the power block works if i) $DNI \times \eta_{opt} > 200 \text{ W/m}^2$ or ii) storage tanks levels are high enough to guarantee power production at design conditions for 1 hour, which occurs for CO₂/CaO tanks levels over 7%. As in the carbonator side CO₂ mass flow varies only slightly because of the ambient temperature, maximum and minimum CO₂ cycle pressures and CO₂ turbines (HPS-TURB and M-TURB in Fig. 1) and CO₂ main compressor (M-COMP) efficiencies are kept constant. Carbonator heat losses ratio is kept constant in off-design to 1% of the heat transferred in the reaction.

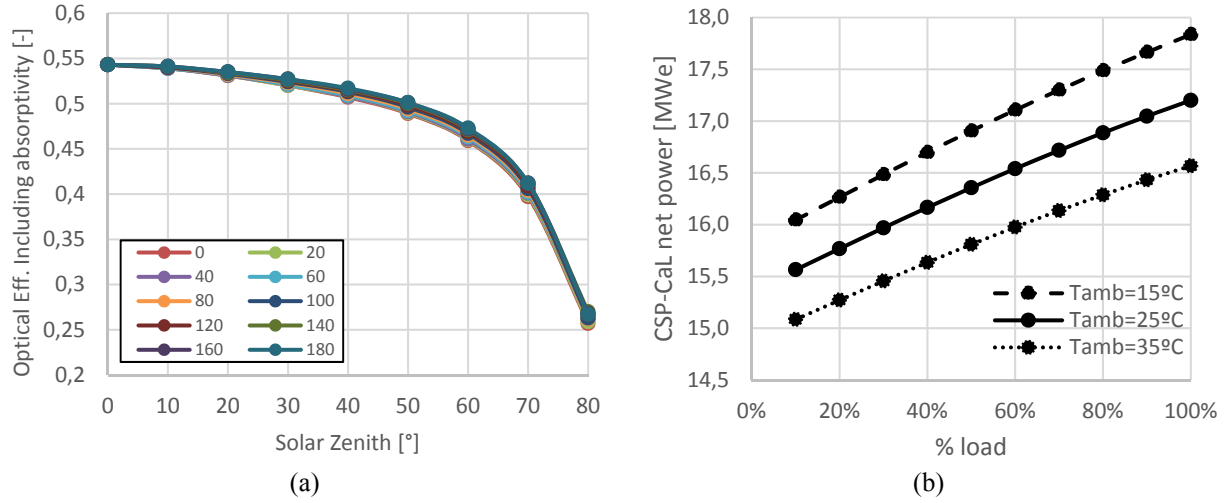


FIGURE 3. (a) Solar field optical performance in off-design conditions as a function of Azimuth and Zenith and (b) CSP-CaL plant net power at partial-load for several ambient temperatures

HOURLY SIMULATION RESULTS

The proposed CSP-CaL plant has been simulated on an hourly basis in order to determine daily profiles for some representative days in Seville (Spain). Solar radiation and ambient temperature data are taken from [18].

As previously indicated, the model assumes a constant power production of the Brayton cycle if solar radiation and storage allow generation. For the simulation, the model assumes that in the first hour of the year (January 01, 1am) both CaO and CO₂ tanks are empty, so power is not produced until solar irradiance reaches the threshold value, which occurs at noon (see Fig. 4a). On the other hand, it is assumed that the CaCO₃ tank is full at the beginning of the year.

Simulation results show that the strategy for power production and the storage tanks capacity proposed lead to a CO₂ cycle capacity factor of 58% (referred to the CO₂ Brayton cycle only, which operates at constant power for 5089 hours/year). The storage tanks size and operation strategy and the solar multiple can be optimized to minimize the cost of electricity taking further information from a techno-economic analysis. Figure 4 shows the levels of the storage tanks in three representative days along the year. CO₂ and CaO tanks levels follow the same trend along the year while the CaCO₃ tank level evolution is opposed. The higher solar irradiation the higher amount of CO₂ and CaO introduced in the stored tanks. Note that the maximum value in each simulated day is quite different and therefore the tank capacity must be carefully designed to match the different requirements along the year.

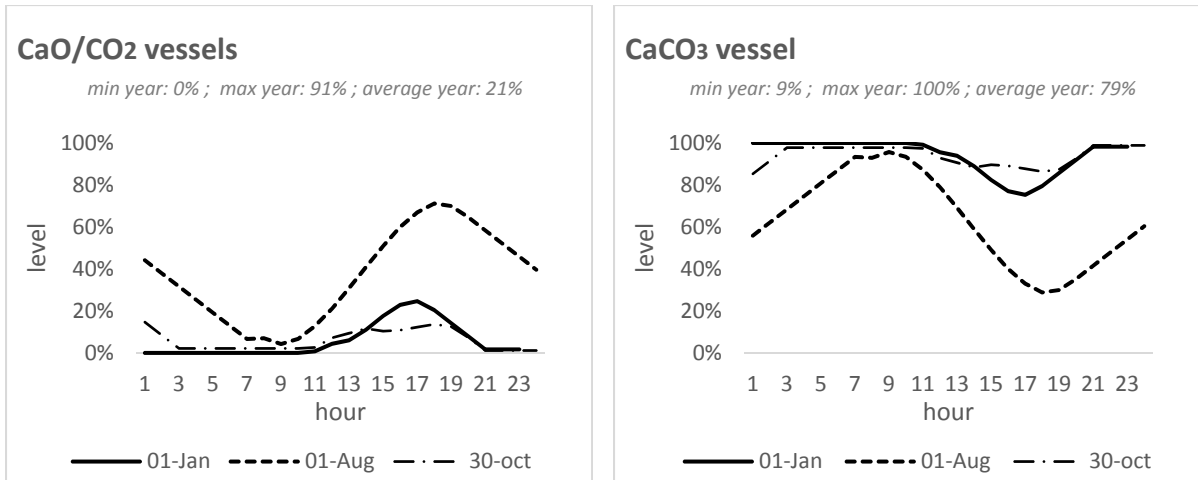


FIGURE 4. Storage tanks levels in three representative days along the year

The capacity factor achieved is similar (or even higher) to the value obtained in commercial solar plants based on molten salts with large storage [19]. Taking into account the higher energy storage density of CaL system in comparison with molten salts [9], higher storage capacity can be reached by using lower volumes tank. For instance, Gemasolar Plant [20], with 15 hours of storage and a capacity factor of 55% requires around 28.47 tonnes/MWh of solar salt [21] while in the CSP-CaL integration the ratio considering the total stored products is 27.69 tonnes/MWh. Remarkably, the mass of stored products in the CSP-CaL process could be further reduced by optimizing the CaL conditions to increase the average CaO conversion [9]. In addition, both the environmental (non-toxicity and wide availability of limestone) and economic aspects (limestone cost around 10\$/tonne [22] instead 893\$/tonne of solar salt [23]) are highly improved by using CaO/CaCO₃ instead molten salts. On this regard, a further economic analysis should be performed to compare the profitability of the whole systems.

Figure 5 shows the net power generation for two representative days of the year. Simulation results show that power generation can be carried out for 9 h on January 1st whereas on August 1st the turbine working hours are prolonged to 23 h. This suggests that an optimized power production pattern throughout the year (instead of considering a constant power production) could achieve a continuous power plant operation for long periods. Further refinements of this control strategy should be pursued though.

As can be seen in Fig. 5, the lowest net power production occurs in the central hours of the day when DNI is the highest due to the high mass flow of CO₂ compressed to be stored at high pressure. Thus, net power production is crucially determined by the ratio of CO₂ mass flow rate exiting the calciner to storage (g_4 in Fig. 1) to the CO₂ mass flow rate that goes directly into the carbonator (g_3). However, different optimized operation criteria should be implemented in an industrial plant to maximize revenues. The daily power production plan will be highly dependent on the variability of the electricity price with the hours of the day and with the day of the week (weekdays or weekend). On this respect, it must be noted that the net design power output of the CO₂ cycle (main CO₂ turbine and main CO₂ compressor) is about 15 MW and therefore the CO₂ cycle load (which may be controlled for example by modifying the rotational speed of the compressor) represents a major degree of freedom.

Main power production and consumption results are also plotted in Fig. 5. Because of the selected operation strategy, power production in the main CO₂ turbine (M-TURB) is constant throughout the year (29.75 MW_e) when power cycle works.

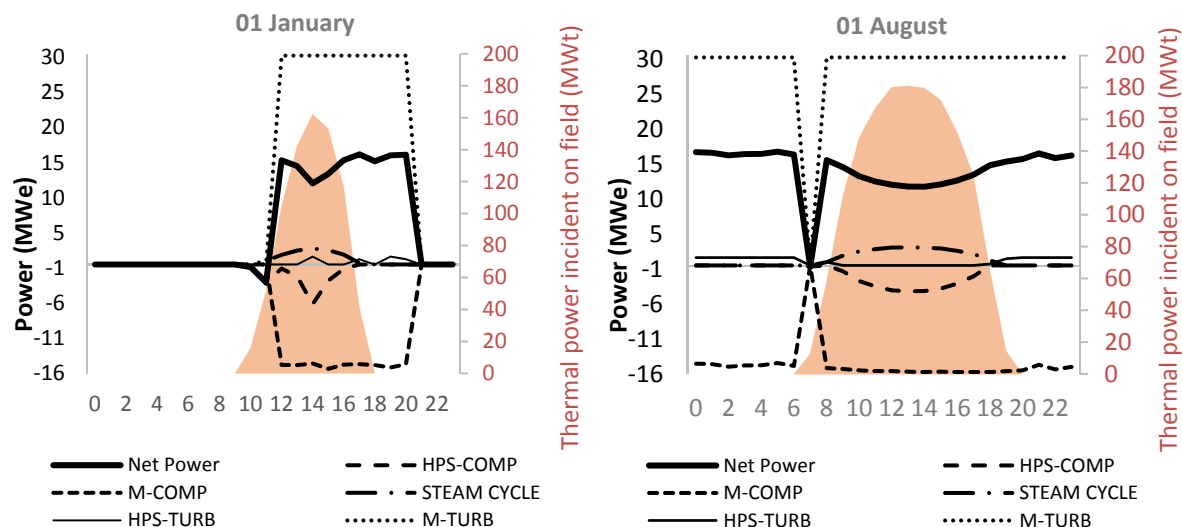


FIGURE 5. Plant simulation results for two representative days of the year. Main power production/consumption along the day are shown.

Main power consumption in the plant is caused by the low-pressure compressor in the Brayton cycle function of the ambient temperature. The high-pressure compressor, which works only in the storage charging step, is responsible for the second largest power consumption in the plant, being the parameter that affects the performance of the system the most. Overall daily solar-to-electric efficiency values of 17.01% and 20.13% are calculated for January and August, respectively. Efficiency is calculated considering the number of products stored, making the plant performance independent from the operating strategy. Differences between winter and summer cases are mainly based on the optical efficiency variation. For comparison, a 18.46% yearly solar-to-electric efficiency is calculated for a molten salts tower plant in the same location [24]. The overall daily solar-to-electric efficiency calculated in the CSP-CaL plant, in addition to higher energy storage capacity, confirms the attractive potential of the Calcium-Looping integration.

CONCLUSIONS

The present work aims at analyzing the potential of a TCES system for CSP plants based on the Calcium-Looping process based on low cost, abundant and non-toxic natural minerals. A model for the off-design calculation of the plant has been developed and a preliminary hour-by-hour simulation considering real radiation data has been carried out. Among the potential benefits of the system, simulation results show that dispatchability could be improved by using the CaL process. The high energy density of the system leads to a plant capacity factor as high as 58% by storing lower mass of products than in commercial molten salt-based CSP plants. Overall daily thermal to power efficiencies of 17.01% and 20.15% are calculated for to representative months of the year in Seville (January and August, respectively), which shows the potential of the technology. Thus, preliminary CSP-CaL results shows benefits compared the current state of the art in terms of capacity factor, solar-to-electric efficiency, energy density, dispatchability and sustainability even in a non-optimized configuration. CO₂ storage conditions, tank sizes and operation strategy will be further studied and optimized in a future work from a techno-economic analysis. Designing the solar receiver for calcination remains as the main challenge for a development of this technology.

ACKNOWLEDGMENTS

This work has been supported by the Spanish Government Agency Ministerio de Economía y Competitividad (MINECO-FEDER funds), contracts CTQ2014-52763-C2-2-R, CTQ2017-83602-C2-2-R and FPI contract granted to Carlos Ortiz Domínguez (BES-2015- 0703149) within the project: Hybrid thermochemical storage of concentrated solar power (CTQ2014-52763-C2-2-R). The research leading to these results has received funding from the European Union's Horizon 2020 research and innovation program under grant agreement No 727348, project SOCRATCES.

REFERENCES

1. National Renewable energy laboratory (NREL), "Concentrating Solar Power Projects," 2017. .
2. T. Shimizu, T. HIRAMA, H. Hosoda, K. Kitano, M. Inagaki, and K. Tejima, "A twin fluid-bed reactor for removal of CO₂ from combustion processes," *Chem. Eng. Res. Des.*, vol. 77, no. 1, pp. 62–68, Jan. 1999.
3. European Solar Thermal Electricity Association (ESTELA), "Solar Thermal Electricity Strategic research agenda 2020-2025," no. december, 2012.
4. R. Chacartegui, A. Alovio, C. Ortiz, J. M. Valverde, V. Verda, and J. A. Becerra, "Thermochemical energy storage of concentrated solar power by integration of the calcium looping process and a CO₂ power cycle," *Appl. Energy*, vol. 173, pp. 589–605, Jul. 2016.
5. W. E. Wentworth and E. Chen, "Simple thermal decomposition reactions for storage of solar thermal energy," *Sol. Energy*, vol. 18, no. 3, pp. 205–214, 1976.
6. G. Flamant, D. Hernandez, C. Bonet, and J. P. Traverse, "Experimental aspects of the thermochemical conversion of solar energy; Decarbonation of CaCO₃," *Sol. Energy*, vol. 24, no. 4, pp. 385–395, 1980.
7. S. E. B. Edwards and V. Materić, "Calcium looping in solar power generation plants," *Sol. Energy*, vol. 86, no. 9, pp. 2494–2503, 2012.
8. A. Alovio, R. Chacartegui, C. Ortiz, J. M. Valverde, and V. Verda, "Optimizing the CSP-Calcium Looping integration for Thermochemical Energy Storage," *Energy Convers. Manag.*, vol. 136, pp. 85–98, 2017.
9. C. Ortiz, M. C. Romano, J. M. Valverde, M. Binotti, and R. Chacartegui, "Process integration of Calcium-Looping thermochemical energy storage system in concentrating solar power plants," *Energy*, vol. 155, pp. 535–551, Jul. 2018.
10. I. Martínez *et al.*, "Review and research needs of Ca-Looping systems modelling for post-combustion CO₂ capture applications," *Int. J. Greenh. Gas Control*, vol. 50, pp. 271–304, 2016.
11. H. M. Kvamsdal, M. C. Romano, L. van der Ham, D. Bonalumi, P. van Os, and E. Goetheer, "Energetic evaluation of a power plant integrated with a piperazine-based CO₂ capture process," *Int. J. Greenh. Gas Control*, vol. 28, pp. 343–355, Sep. 2014.
12. National Renewable energy laboratory (NREL), "SolarPILOT (Solar Power tower Integrated Layout and Optimization Tool)." .
13. J. S. Kim, A. Kumar, and C. Corsi, "Design boundaries of large-scale falling particle receivers," *AIP Conf. Proc.*, vol. 1850, pp. 1–9, 2017.
14. E. Casati, F. Casella, and P. Colonna, "Design of CSP plants with optimally operated thermal storage," *Sol. Energy*, vol. 116, pp. 371–387, 2015.
15. A. Bayon *et al.*, "Techno-economic assessment of solid-gas thermochemical energy storage systems for solar thermal power applications," *Energy*, vol. 149, pp. 473–484, 2018.
16. Thermoflow Inc., "Thermoflex, Fully-flexible design and simulation of conventional steam plants, combined cycles, and other thermal power systems." Southborough, MA, USA.
17. A. Patnode, "Simulation and performance evaluation of parabolic trough solar power plants," *Univ. Wisconsin-Madison*, vol. Master, pp. 5–271, 2006.
18. European Commission, "Photovoltaic geographical information system (PVGIS)." .
19. IRENA, "Renewable Power Generation Costs in 2017," 2018.
20. Torresol Energy, "GemSolar plant." [Online]. Available: <http://torresolenergy.com/en/gemasolar/>. [Accessed: 01-Apr-2018].
21. J. I. Burgaleta, S. Arias, and D. Ramirez, "GemSolar: The First Tower Thermosolar Commercial Plant with Molten Salt Storage System," *SolarPACES Int. Conf.*, no. Sept., pp. 11–14, 2012.
22. P. Lisbona, A. Martínez, Y. Lara, and L. M. Romeo, "Integration of carbonate CO₂ capture cycle and coal-fired power plants. A comparative study for different sorbents," *Energy and Fuels*, vol. 24, no. 1, pp. 728–736, 2010.
23. C. Parrado, A. Marzo, E. Fuentealba, and A. G. Fernández, "2050 LCOE improvement using new molten salts for thermal energy storage in CSP plants," *Renew. Sustain. Energy Rev.*, vol. 57, pp. 505–514, 2016.
24. S. Polimeni, M. Binotti, L. Moretti, and G. Manzolini, "Comparison of sodium and KCl-MgCl₂ as heat transfer fluids in CSP solar tower with sCO₂ power cycles," *Sol. Energy*, vol. 162, no. January, pp. 510–524, 2018.